Cent. Eur. J. Phys. • 6(2) • 2008 • 205-210
DOI: 10.2478/s11534-008-0050-0

VERSITA

Central European Journal of **Physics**

Coherent control for the spherical symmetric box potential in short and intensive XUV laser fields

Research Article

Imre F. Barna[1]*, Péter Dombi[2]

1 Atomic Energy Research Institute of the Hungarian Academy of Sciences, (KFKI-AEKI), H-1525 Budapest, P.O. Box 49, Hungary

2 Research Institute for Solid State Physics and Optics of the Hungarian Academy of Sciences, (KFKI-SZFKI) H-1525 Budapest, P.O. Box 49, Hungary

Received 20 September 2007; accepted 14 February 2008

Abstract: Coherent control calculations are presented for a spherically symmetric box potential for non-resonant two photon transition probabilities. With the help of a genetic algorithm (GA), the population of the excited states are maximized and minimized. The external driving field is a superposition of three intensive extreme ultraviolet (XUV) linearly polarized laser pulses with different frequencies in the femtosecond duration range. We solved the quantum mechanical problem within the dipole approximation. Our investigation clearly shows that the dynamics of the electron current has a strong correlation with the optimized and neutralizing pulse shape.

PACS (2008): 32.80.Qk, 32.80.Fb, 32.80.Wr

Keywords: coherent control • free-electron laser • genetic algorithm

© *Versita Warsaw and Springer-Verlag Berlin Heidelberg.*

1. Introduction

Coherent control has become a routine procedure, in physics and chemistry, to optimize and govern light-matter interaction processes in atomic and molecular systems [1, 2]. The original and most commonly known coherent control methods are realized by envelope and phase shaping of visible or near-IR femtosecond laser pulses. Thereby the corresponding electronic transitions, induced by these pulses, can be controlled and enhanced in a very powerful manner.

There is enormous future potential in this method outside the traditional scope of femtochemistry. It is well known that schemes for the generation of extreme ultraviolet (XUV) radiation, by the process of high harmonic generation (HHG), are suitable for the production of light pulses with a duration of less than a femtosecond. As a result, attosecond metrology and spectroscopy based on HHG sources are becoming more and more widespread methods in atomic physics [3, 4]. The first attosecond experiments used light pulses from the HHG gas jet as they emerged, sometimes after some dispersion control, to attempt to preserve the original shape of the XUV pulse [3, 4]. As a more sophisticated form of phase shaping, XUV radiation chirped multilayer structures were recently considered and used for XUV pulse optimization [5–7]. How-

*E-mail: barnai@sunserv.kfki.hu

ever, these efforts are only aimed at compensating for the chirp of the XUV pulses, thus making the XUV pulse duration shorter. Such passive methods are satisfying until one demands to achieve, for a given spectrum, the shortest possible attosecond pulses. If one wants to use coherent control methods at these wavelengths more complex phase control schemes are needed.

Several groups have become engaged in transforming coherent control schemes to XUV light-matter interactions in recent years. Since standard methods involving control of the spectral intensities and/or phases (by the use of spatial light modulators, acousto-optic programmable dispersive filters) are not directly applicable in the XUV spectral domain other methods have emerged. i) It seemed straightforward to perform phase and amplitude shaping on the infrared laser pulse with standard coherent control setups first. The spectral and temporal properties of the HHG radiation generated by this pulse can thus be influenced. This option has mainly been exploited to maximize harmonic conversion efficiency and to enhance conversion to a given harmonic [8–10]. More recently, as a further step towards XUV coherent control, Pfeifer *et al.* have realized control of the branching ratio of the dissociative photoionization of sulfur hexafluoride by adaptive shaping of the HHG generating infrared field [11]. ii) Other groups use wavefront or fiber mode shaping methods to enhance harmonic yield, for a given harmonic, in the HHG process [12–15]. This does not involve temporal shaping of the pulse to first order, however, it proved to be powerful for enhancing the harmonic yield. iii) It is less straightforward to achieve phase shaping of the XUV beam, after the high harmonic generation process, to realize the desired temporal shaping effect. However, very recently, Strasser *et al.* managed to construct such a scheme and thereby control the coherent transients in a He atom[16]. Another option for direct adaptive phase modulation in the XUV spectral domain would be the application of deformable mirrors known from visible/near IR technology. To our knowledge, efforts involving such technology have not been published.

XUV radiation sources other than HHG also have to be considered. Free electron laser beam-lines also open up new horizons in femtosecond X-ray research by targeting parameter regimes currently unavailable to laser-driven XUV/X-ray sources [17–19]. Unfortunately, these sources are not particularly suitable for coherent control applications due to their limited temporal coherence[1]. Prompted by these developments more general, purely theoretical, studies on coherent control in the XUV domain also emerged [20, 21]. One of us has also tried to answer related questions by theoretically investigating a non-resonant two-photon transition in He (1s1s) - (1s3s) with shaped XUV pulses [20]. These calculations, however, lacked insight into the fundamental physical background of the control process. Therefore, in this paper, we investigate the control process further with numerical tools for a more simple model system, a spherical box potential, and a simplified ansatz for the genetic algorithm. The motion of an electron was investigated in a spherically symmetric square well potential driven by a linearly polarized XUV laser pulse. We solved the time-dependent Schrödinger equation with our simplified coupled-channel method which was successfully applied for more complex laser-atom interaction problems [22]. We chose spectral intensities and phases as the optimization parameters for coherent control. Even though a corresponding experimental scheme does not yet exist, our approach provides a very general treatment of the problem. As a next step, we apply the genetic algorithm (GA)[2] as the optimization procedure to create the best interacting, or most indifferent pulses (we call it neutralization), for state selective excitation. A detailed analysis about the evolutionary algorithms in optimal control studies was presented in [23]. Further exhausted details about different learning algorithms can be found in [24]. Our results show that the wave packet dynamic, the center-of-mass of the electron current, is strongly correlated with the shape of the laser pulse. This gives us a physical interpretation for the control mechanism for this model potential problem. Section 2 shortly outlines the theoretical background of our model, followed by a compact description of the GA. Section 3 presents our results with an explanation. Atomic units [a.u.] are used through the paper unless otherwise indicated.

2. Theory

We solve the general time-dependent problem with our simplified coupled-channel approach to describe controlled laser driven excitation processes in the spherically symmetric box potential. The original method can be found in our former studies[3] [22, 25]. For the expansion coefficients of the time-dependent wavefunction the following

[1] *DESY homepage, http://xfel.desy.de/technical_information/photon_beam_parameter.*

[2] *D.L. Carroll, Free Genetic Algorithm Driver http://cuaerospace.com/carroll/ga.html.*

[3] *http://geb.uni-giessen.de/geb/volltexte/2003/1036*

differential equation system holds

$$\frac{da_k(t)}{dt} = -i\sum_{j=1}^{N} V_{kj}(t)e^{i(E_k-E_j)t}a_j(t), \quad (k=1,...,N), \quad (1)$$

where E_k and E_i are the eigenvalues of the box potential, and will be specified later. The coupling matrix elements

$$V_{kj}(t) = \langle \Phi_k | \hat{V}(t) | \Phi_j \rangle. \quad (2)$$

are taken with the well known eigenfunctions of the box potential. The probabilities for transitions into final excited states j after the pulse are simply given by

$$P_j = |a_j(t=T)|^2, \quad (3)$$

where T is the duration of the pulse. To get the total excitation probability the corresponding channels P_j must be summed up. When a state selective excitation probability is controlled, then only the corresponding channel is considered. We have to mention that the box potential also has a continuous spectra, this can be interpreted as the ionization spectra. In the following we concentrate on non-resonant two-photon excitation processes and neglect three-photon ionization yields which have negligible contributions in similar atomic systems [20]. We restrict ourselves to linearly polarized laser pulses parallel to the z-axis. The length gauge within the dipole approximation is applied

$$V(t) = -\mathbf{E}(t)\cdot\mathbf{r}. \quad (4)$$

To understand the control mechanism we took a simple model and investigated the three-dimensional, spherically symmetric, square-well potential. With the help of the width 'b' and the depth '$-V_0$' (which are the only two parameters of this potential) the number of bound states can be fixed. We tune these parameters in such a way ($b = 5$ a.u., $V_0 = 5$ a.u.) that only four bound states exist. The four states have different angular momenta from zero up to three. A detailed analysis of the problem can be found in any textbook [26]. The wave functions inside the box potential are the well known spherical Bessel functions and the energies can be found as solutions of different transcendental equations. The four bound states have the following energies: $E_{\ell=0} = -3.6$ a.u., $E_{\ell=1} = -1.85$ a.u., $E_{\ell=2} = -0.36$ a.u., $E_{\ell=3} = -0.05$ a.u.

For the external driving field strength, we add three different frequencies and use a $\sin^2$ envelope,

$$\vec{E}(t) = E_n \cdot \sin^2\left(\frac{\pi t}{T}\right)[a_1\sin(\omega_1 t+\delta_1)+ a_2\sin(\omega_2 t+\delta_2)+a_3\sin(\omega_3 t+\delta_3)]\vec{e}_z, \quad (5)$$

where the frequencies are fixed and the three amplitudes $a_{1,2,3}$ and phases $\delta_{1,2,3}$ are the free parameters optimized through the GA [21].

Here we choose spectral intensities and phases as the optimization parameters for coherent control, thus following standard schemes used for coherent control with visible light pulses. This would imply that a spatial light modulator, or a similar device, exists that is capable of controlling the spectral phases and intensities of the XUV beam in a setup similar to the standard 4f-scheme. Even though such a device does not exist currently, our method provides a much more general approach than just optimizing chirp parameters. Using this methodology, more complex pulse shapes can be simulated than provided by low-order chirps and more general conclusions can be drawn that will be useful for planning future experimental schemes.

For ω_1 we took a quasi resonant two-photon frequency: $(E_{\ell=2} - E_{\ell=0})/2 \approx \omega_1 = 1.52$ a.u. The resonant frequency is 1.62 a.u., therefore when ω_1 is closer to resonance, all pulses excite the system with a large probability ($P_2 >$ ten percent range) and the electron dynamics between the optimized and neutralized cases have the same properties. On the other hand, if ω_1 is much further from resonance, then the optimization can not give us enough excitation, and the system practically remains in the ground state. For the two other frequencies we took $\omega_2 = 1.40$ a.u. and $\omega_3 = 1.85$ a.u. The GA freely varies the phases $|\delta_{1,2,3}| \leq \pi$ and the amplitudes $|a_{1,2,3}| \leq 2$. This approach permits combinations where the contribution of the quasi resonant frequency is suppressed, letting the off-resonant frequencies to evolve their effect. Contrary to the widely used phase modulation, this pulse fabrication mechanism does not conserve pulse energy, and this is why all pulses have to be renormalized to a reference pulse

$$\int_0^T |\vec{E}(t)|^2 dt = 25.13\, a.u. \quad (6)$$

For the reference pulse we took the quasi resonant frequency only, $\omega = 1.52$ a.u., with a large field strength $E_0 = 0.6$ a.u. and a $T = 400.53$ a.u. pulse duration; E_n is the normalization constant Eq. (5). This parameter set gives us the massive excitation probabilities which are required for further investigation.

For time propagation we use a Runge-Kutta-Fehlberg method of fifth order embedding an automatic time step regulation. Despite the non-unitarity of the Runge-Kutta-Fehlberg method, the adaptive step-size correction can suppress the numerical error to less than 10^{-8} during the time propagation [25, 27].

As an optimization procedure we used the celebrated genetic algorithm which works in the following way. The GA represents each possible solution, or individual, with

a string of bits, termed a chromosome. For example two possible phases are represented as [01101101]. (For the sake of clarity we assume that each parameter can only take $2^3 = 8$ values in this example.) The first generation of individuals is selected randomly. Typically, we use a population of size of 20 which is about a factor of three larger than the number of the optimisable variables. For each generation, the following steps are carried out: (i) all the individuals are evaluated and assigned a fitness value. In our case it means that we calculate the ionization or state selective excitation probability resulting from each parameter configuration and call it the fitness value for that configuration. The next generation of individuals is chosen by applying three GA operators: selection, mutation and crossover. (ii) The selection operator chooses which of the individuals from the present generation will be transfered to the next generation. The individuals are ranked according to their fitness, and then selected randomly with a certain probability based on the fitness. A very fit individual thus receives a high probability and can be selected many times, while low-fitness individuals may not be selected at all. (iii) The mutation operator, which is used very seldomly, selects a few individuals and replaces one (randomly selected) bit in a chromosome randomly by 0 or 1 (e.g. creating the chromosomes [11010100] from [11000000].) (iv) The crossover operator takes two individuals at a time and exchanges part of their chromosomes. For example two chromosomes [01101000] and [01001110] can create the chromosomes [01101110] and [01001000]. The use of the mutation and crossover operators ensures that the GA does not became fixed in a local minimum or maximum. The fittest individuals, however, always survive to the next generation in what is called elitism. Steps (i)-(iv) are repeated until no new solutions appear between two consecutive generations. In the optimizations presented in this work, the GA typically converges after 40-70 generations.

3. Results

The laser field has six free parameters that have to be optimized through the control process. The GA also needs further technical parameters [21]. We used 20 different pulses per generation (population size) and let the process run through 60 generations to achieve convergence. This means that $20 \times 60 = 1200$ different pulses were checked to find the most favorable. Using permutation probability ($\approx$ 1/population size) = 0.05, crossover probability = 0.4 and creeping probability = 0.12 gave us good convergence and gain, matching the commendation of the routine [21]. We found the algorithm stable and robust against slight

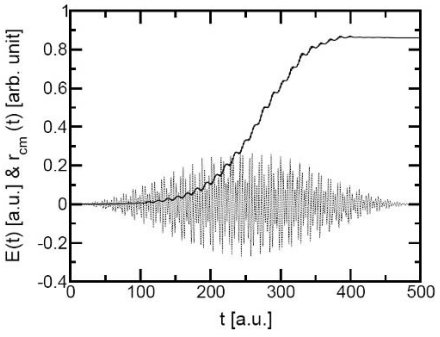

Figure 1. The electric field strength E(t) of the optimized pulse (dashed line) with the corresponding center of mass of the electron current r_{cm}(t) solid line)

parameter variations. Further slight "blind-changing" of these parameters may give some extra 10-15 percent gain, but the identified mechanism will not be changed.

The GA makes it possible to carry out two different kinds of optimization calculations, first the maximization of the excitation probabilities (we call it optimization) and secondly minimization (we call it neutralization) when the transition probabilities are minimized. To interpret the control mechanism, both of these calculations had to be done. The neutralization calculation may attract large interest in future FEL experiments where on one side the maximal field strength is used but on the other side the field must not interact with the resonator causing any damage. The optimized P_2 transition probability for the pulse given above is 2.3×10^{-3}, compared to the neutralized probability of 2.8×10^{-5}, which is a factor of 82 smaller. The parameters of the optimized pulse are: $a_{1,2,3}$ $[1.57, 0.68, 1.38]$ $\delta_{1,2,3}[0.45, -0.88, 0.52]$ and for the neutralizing pulse: $a_{1,2,3}[1.17, 1.68, 0.82]$, $\delta_{1,2,3}[-0.52, 0.66, 0.12]$. Note that these pulses are not the absolute best or darkest pulses, but optimized enough to show the feature of the coherent control mechanism. To find some physical interpretation for our control results, we investigated the dynamics of the electron wave packet. We calculated the time-dependent current of the electron through the following formula:

$$\mathbf{j}(\mathbf{r}, t) = \Psi(\mathbf{r}, t)^* \vec{\nabla} \Psi(\mathbf{r}, t), \tag{7}$$

for the time-dependent wave function we used the usual form:

$$\Psi(\mathbf{r}, t) = \sum_{\ell=0}^{3} a_\ell(t) \Phi_\ell(\mathbf{r}) e^{-iE_\ell}, \tag{8}$$

where

$$\Phi_\ell(\mathbf{r}) = \left(\frac{\pi}{2r}\right)^{\frac{1}{2}} \cdot J_{\ell+\frac{1}{2}}(rk) Y_{\ell,0}(\theta, \varphi). \tag{9}$$

The radial part $\sqrt{\pi/2r}J_{\ell+0.5}(rk)$ is the spherical Bessel function of the first kind, (usually noted $j_\ell(rk)$, however this may lead to miss-understanding when using the same letter for electron current) $J_{\ell+\frac{1}{2}}(rk)$ is the ordinary Bessel functions of half-odd-integer order and $Y_{\ell,0}(\theta,\varphi)$ is the usual spherical harmonic.

The current is a complicated quick oscillating function, so it is difficult to observe its correlation with the laser field, thus we introduce the center-of-mass coordinate of the electron current

$$r_{cm}(t) = \frac{\int j(r,t)\cdot r dr}{\int j(r,t) dr}, \tag{10}$$

which is a pure time-dependent number. We concentrate on the radial current component only, skipping the vector notation. It is easy to see that the center-of-mass of the current is a bound function of time. Before the laser pulse, without any external field, the system is in the $\ell = 0$ ground state with a wave function proportional to $\frac{\sin(rk)}{rk}$. This function is maximal at zero and has a strong decay, hence the center-of-mass coordinate is close to zero. On the other hand the wave functions of the excited states are higher order Bessel functions having a zero at the origin and maximum at $r = 5.0$ a.u. Inside a laser pulse the electron is in a mixed quantum state. With a linear scaling, we may identify the minimum of the current with zero and the maximum to a number comparable with the peak field intensity. Fig. 1 shows the electric field strength of the optimized pulse together with the corresponding electron current function. Beyond the $\sin^2$ envelope shape and the carrier oscillation, an extra modulation can be found with a quasi periodic time of $\tau \approx 14$ a.u. This property of the pulse is a beat phenomena. The well-known addition theorem says:

$$\sin(\alpha) + \sin(\beta) = 2\sin\left(\frac{\alpha+\beta}{2}\right)\cos\left(\frac{\alpha-\beta}{2}\right), \tag{11}$$

which means that adding two different frequencies with the same amplitude and the same phase gives us a completely new amplitude modulated signal with the beat time of: $\tau_{beat} = \frac{\pi}{|\alpha-\beta|/2}$. By checking the parameters of the optimized pulse, we found that ω_2 and ω_3 have approximately the same amplitude and the same phase, giving us $\tau = 13.96$ a.u. The amplitude modulation is not maximal due to the existence of ω_1.

Let's investigate the current now. It is clear to see that, for $t > 150$ a.u., the current continously gains between two neighboring beat oscillation minima and has a short plateau at the vicinity of the minima. This behavior can be explained as a resonance phenomenon, where the electron absorbs energy from the laser pulse at each intensity growth. The time-dependent center-of-mass of the electron current shows two kinds of oscillations. The slower oscillation follows the envelope of the pulse (we call it envelope oscillation) and a much quicker, but smaller, oscillation follows the carrier of the pulse (we call it carrier oscillation). The work of Kosloff *et al.*[28] proves that there is a $\pi/2$ phase shift between the optimal pulse and the time dependent wave function overlap. Fig. 2 shows a magnified part of the field strength of the optimized pulse, together with the overlap of the time-dependent ground state wave function and the $\ell = 2$ wave function through the dipole operator.

$$O(t) = i\langle\Psi_{\ell=2}(\mathbf{r},t)|\hat{d}|\Psi_{\ell=0}(\mathbf{r},t)\rangle. \tag{12}$$

We optimized to a two photon transition, thus the overlap function has double periodicity. The vertical line between the field strength and the overlap shows a $\pi/2$ phase shift. When the electric filed strength has a local minimum, or maximum, then the overlap function's carrier oscillation has a zero transition crossing the envelope function. Due to the different time, the amplitude scale of the envelope and the carrier oscillation, this effect is hard to see.

Finally, Fig. 3 presents the electric field strength of the neutralizing pulse together with the corresponding electron current function. Contrary to the optimized pulse, the current has local maximum when the envelope reaches its minimum and vice versa. The system decays with growing field strength. This property of the current can be explained as a fucntion of off-resonant dynamics, field strength and electron movement. The beat oscillation comes into play again $\tau_{beat} \approx 50/3 \approx 16.6$ a.u., this is hard to identify because $\tau_{\omega_1-\omega_3} = 19.03$ a.u. and $\tau_{\omega_2-\omega_3} = 13.96$ a.u. No unambiguous correlation could be found between the second quick oscillation of the current and the laser field. It is important to mention that different optimized and neutralizing pulses, and their corresponding currents, were examined from the last generation and all showed the same properties as analyzed above.

4. Summary and outlook

We presented coherent control calculations for the spherically symmetric box potential in short intensive XUV laser pulses. With the help of a GA we maximized and minimized two-photon non-resonant probabilities. We found that the center-of-mass of the electron current is highly correlated with the envelope of the exciting laser pulse. The field of optimized laser pulses force the quiver motion on the electron wave packet to be in-phase with the envelope of the pulse. However, neutralized pulses force the

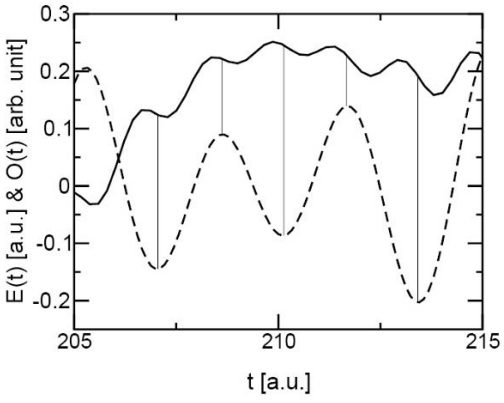

Figure 2. The $\pi/2$ phase shift between the optimized time-dependent wave function overlap O(t) (solid line) and the electric field strength E(t) of the laser pulse (dashed line)

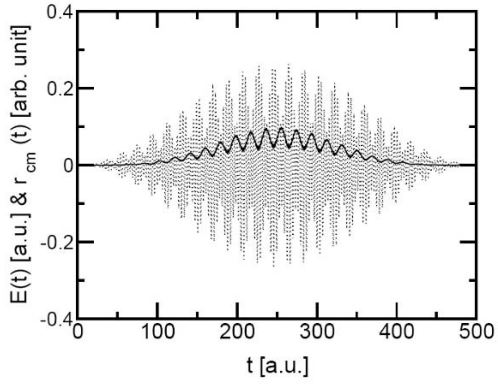

Figure 3. The electric field strength E(t) of the neutralized pulse (dashed line) with the corresponding center of mass of the electron current r_{cm}(t) solid line)

electron to follow a motion which is out-of-phase relative to the envelope.

It is basically possible to implement our method, for many-electron atoms, to investigate and control ionization processes. Such works are in progress. Experimental coherent control experiments are carried out with visible or infrared lights nowadays. Our calculations were done in the hope that the rapid development of laser technology will make such schemes realizable in the near future. Some results of the first pioneering experiments are already available [16] with tabletop laser systems, moreover such control schemes are also applicable in free-electron-laser beam-lines delivering femtosecond XUV pulses.

Acknowledgments

We thank Prof. A. Becker and Prof. J.M. Rost for fruitful discussions and constructive ideas. We acknowledge support from the Hungarian Scientific Research Fund (OTKA Project F60256). P. D. was also supported by the Bolyai Fellowship of the Hungarian Academy of Sciences.

References

[1] A.M. Weiner, Prog. Quant. Electr. 19, 161 (1995)
[2] T. Brixner, N.H. Darmrauer, G. Gerber, Advances in Atomic, Molecular, And Atomic Physics 46, 1 (2001)
[3] P. Agostini, L. DiMauro, Rep. Prog. Phys. 76 813 (2004) and references therein.
[4] P.B. Corkum, F. Krausz, Nature Phys. 3, 381 (2007) and references therein.
[5] A.S. Morlens et al., Opt. Lett. 31, 1558 (2006)
[6] E. Gustafsson et al., Opt. Lett. 32, 1353 (2007)
[7] M. Schultze et al., New J. Phys. 9, 243 (2007)
[8] R. Bartels et al., Nature 406, 164 (2000)
[9] D.H. Reitze et al., Opt. Lett. 29, 86 (2000)
[10] T. Pfeifer et al., Appl. Phys. B 80, 277 (2005)
[11] T. Pfeifer et al., Opt. Express 15, 3409 (2007)
[12] C. Altucci et al., Phys. Rev. A 61, 021801 (2000)
[13] P. Villoresi et al., Opt. Lett. 29, 207 (2004)
[14] D. Yoshitomi et al., Appl. Phys. B 78, 275 (2004)
[15] D. Walter et al., Opt. Express 14, 3433 (2006)
[16] D. Strasser et al., Phys. Rev. A 73, 021805(R) (2006)
[17] H. Wabnitz et al., Nature 420, 482 (2002)
[18] R. Santra, C.H. Greene, Phys. Rev. Lett. 91, 233401 (2003)
[19] E.L. Saldin, E.A. Schneidmiller, M.V. Yurkov, Phys. Rev. Spec. Top.–Ac. 9, 050702 (2006)
[20] I.F. Barna, Eur. Phys. J. D 33, 307 (2005)
[21] J.J. Carrera, S. Chu, Phys. Rev. A 75, 033807 (2007)
[22] I.F. Barna, J. Wang, J. Burgdörfer, Phys. Rev. A 73, 023402 (2006)
[23] D. Zeidler, S. Frey, K.-L. Kompa, M. Motzkus, Phys. Rev. A 64, 023420 (2001)
[24] P. Mars, J.R. Chen, R. Nambair, Learning Algorithms (CRS Press Inc., 1996)
[25] I.F. Barna, Ionization of helium in relativistic heavy-ion collisions, Doctoral thesis (University Giessen, Giessen, Germany, 2002)
[26] L.I. Schiff, Quantum Mechanics (McGraw-Hill, 1955) 76
[27] I.F. Barna, N. Grün, W. Scheid, Eur. Phys. J. D 25, 239 (2003)
[28] R. Kosloff et al., Chem. Phys. 139, 201 (1989)